Bull. Soc. R. Sci. Liège, 2024, **93**(2), 719–726 *Peer-reviewed conference paper*
doi:10.25518/0037-9565.11853

Prompt Emission Properties of GRB 200613A

Ankur GHOSH[1,*], Kuntal MISRA[1] and Dimple [1,2]

[1] Aryabhatta Research Institute of observational sciences, Manora Peak, Nainital 263 001, India
[2] Department of Physics, Deen Dayal Upadhyaya Gorakhpur University, Gorakhpur-273009, India
[*] Corresponding author: ghosh.ankur1994@gmail.com

Paper presented at the 3rd BINA Workshop on "Scientific Potential of the Indo-Belgian Cooperation", held at the Graphic Era Hill University, Bhimtal (India), 22nd–24th March 2023.

Abstract

We study the prompt emission properties of the long duration GRB 200613A using *Fermi*–Gamma-Ray Burst Monitor (GBM) and Large Area Telescope (LAT) data. The prompt emission light curve of GRB 200613A reveals a strong peak emission up to $\sim$ 50 s after the burst accompanied by an extended emission up to $\sim$ 470 s similar to that seen in ultra-long GRB light curves. The time-integrated spectroscopy shows that the Band function best fits the main emission episode, and the extended emission follows the power-law behaviour because of poor count rates. Due to its high isotropic energy and low peak energy, GRB 200613A lies at the extreme end in both the $E_{\rm p}$–$E_{\rm iso}$ and $E_{\rm p}$–T_{90} plots. In addition to the GBM detection, the *Fermi*-LAT detected the highest energetic photons of 7.56 GeV after 6. ks since burst, which lies beyond the maximum synchrotron energy range.

Keywords: Gamma-Ray Bursts, *Fermi*-GBM/LAT, prompt emission

1. Introduction

Gamma-Ray Bursts (GRBs) are extremely energetic transient events in the Universe, releasing colossal amounts of energy which can last from a few milliseconds to several thousand seconds. Traditionally, GRBs are classified into two sub-categories (long and short) based on their T_{90} duration (the time interval during which 90% of the total fluence has been estimated; Kouveliotou et al. 1993). Although this duration-based classification is sensitive to many factors, it is still valid to a certain extent. In the last decade, a subset of GRBs was detected with duration $>$ 500 s, known as ultra-long GRBs (Stratta et al., 2013; Levan et al., 2014). The unique and relatively rare sub-class of GRBs typically consists of a shorter main episode and an extended quiescent emission, attributed to late-time central engine activity (Zhang et al., 2014). Their extended duration far exceeds typical long GRBs, posing intriguing questions about the physical mechanisms responsible for such long-lasting bursts (Boër et al., 2015).

Table 1: Properties of GRB 200613A.

Parameters	Values	References
T_{90} duration (s)	470	Bissaldi et al. (2020)
Redshift	1.22	de Ugarte Postigo et al. (2021)
Fluence (erg cm^{-2})	$(4.10 \pm 0.05) \times 10^{-5}$	Bissaldi et al. (2020)
$E_{\rm iso}$ (erg)	$1.37^{+0.05}_{-0.04} \times 10^{53}$	This work
$E_{\rm p}$ (keV)	115 ± 5	This work

Although multiple empirical models such as the Band function (Band, 1997), the cut-off power-law (CPL), the smoothly-broken power-law (SBPL), and the black body (BB) can explain the prompt emission mechanism in GRBs but it is still poorly understood. Recent studies by Burgess et al. (2020) and Acuner et al. (2020) have shown that physical models like synchrotron and photospheric emission could be the primary components of prompt emission. With the detection of ultra-long GRBs, it is vital to study the prompt emission mechanism and the characteristics of the long-lived central engine.

GRB 200613A ($z = 1.22$) lies at the boundary between long and ultra-long sub-classes with the burst duration ~ 470 s. It has a strong emission component up to ~ 50 s and an extended emission (from 200 s to 470 s having a signal-to-noise ratio of 3.5σ), almost resembling the temporal structure of ultra-long GRBs. The key properties of GRB 200613A are outlined in Table 1. This study presents a comprehensive prompt emission study of GRB 200613A using the *Fermi* data and compares it with other GRBs. The observations and data reduction are briefly described in Sect. 2. The results obtained are presented in Sect. 3. A concise summary of this work is presented in Sect. 4. We assume flat cosmology throughout the paper with $H_0 = 71\,{\rm km\,s^{-1}\,Mpc^{-1}}$, $\Omega_m = 0.27$, and $\Omega_\lambda = 0.73$ (Komatsu et al., 2011).

2. *Fermi* Data Reduction and Analysis

2.1. GBM light curve and spectra

GRB 200613A was triggered and located by *Fermi*-GBM at 05:30:08 UT on June 13, 2020 (Fermi GBM Team, 2020). *Fermi*-LAT detected the GRB at the same time as the boresight angle at the time of GBM trigger was 25° (Ohno et al., 2020). The GBM data was taken from the public data archive of *Fermi* satellite. We reduced the GBM data following the standard process of `GBM Data Tools` and `GTBurst`. We picked the two NaI0 and NaI1 detectors for our further analysis as the count rates are maximum and observing angles are minimum for those detectors. The angle constraint is imposed because the systematic uncertainty at larger angles becomes significant. The BGO0 detector was preferred over BGO1 because of the same reason. Figure 1 shows the GBM light curves in the (50–300) keV, (300–900) keV, and (8–900) keV energy ranges. The prompt emission light curve in (50–300) keV exhibits a bright emission from T_0 to $T_0 + 50$ s, followed by a comparatively weaker emission up to 470 s since the explosion. The weaker extended emission is not evident in the (300–900) keV light curve.

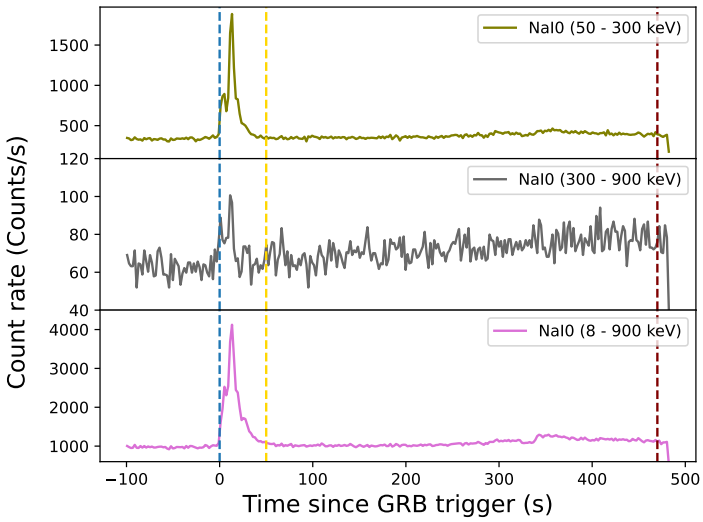

Figure 1: Multichannel light curve of GRB 200613A of NaI0 detector in three different energy bins (50–300 keV, 300–900 keV, and 8–900 keV). The dashed vertical gold line indicates the strongest peak emission up to 50 s. The T_{90} duration of the GRB is indicated by the maroon dashed line.

To investigate the radiation mechanism associated with the prompt emission of GRB 200613A, we performed a time-integrated spectral analysis using threeML (Vianello et al., 2017). The spectral analysis was carried out for the NaI (8–900 keV) and BGO (200-30000 keV) detectors. For fitting the bright phase of the GRB (up to 50 s since the burst), multiple phenomenological models such as the Band function, CPL, SBPL, and PL+BB were considered. We adopted the Bayesian parameter estimation technique using the "dynesty-nested" sampler in threeML to estimate the best-fit value. Depending on the Akaike Information Criterion (AIC), the Bayesian Information Criterion (BIC; Kass and Rafferty, 1995), and the log-likelihood for individual models, the Band function is the best-suited model for this period. The best-fitted parameters of each model are given in Table 2. Due to the poor count rate in the extended emission region, only the power law model can provide a better fit to the spectra.

Table 2: Results of spectral analysis of GRB 200613A based on *Fermi* - GBM data.

Model parameters for the peak interval (9–17 s)					
Band parameters	**Best-fit value**	**CPL parameters**	**Best-fit value**	**SBPL parameters**	**Best-fit value**
α	$-0.95^{+0.02}_{-0.02}$	index	$-0.96^{+0.02}_{-0.02}$	α	$-1.07^{+0.02}_{-0.02}$
$E_{\rm p}$ (keV)[1]	$+151.30^{+3.00}_{-3.20}$	$E_{\rm c}$ (keV)[2]	$+148.00^{+6.00}_{-5.00}$	$E_{\rm b}$ (keV)[3]	$+223.00^{+21.00}_{-19.00}$
β	$-3.79^{+0.42}_{-0.32}$			β	$-4.01^{+0.23}_{-0.28}$
BIC	+3749.41	BIC	+3778.81	BIC	+3755.25
Log(Z)[4]	−811.86	log(Z)	−813.05	log(Z)	−812.82

[1] Peak energy; [2] Cutoff energy; [3] Break energy; [4] Evidence

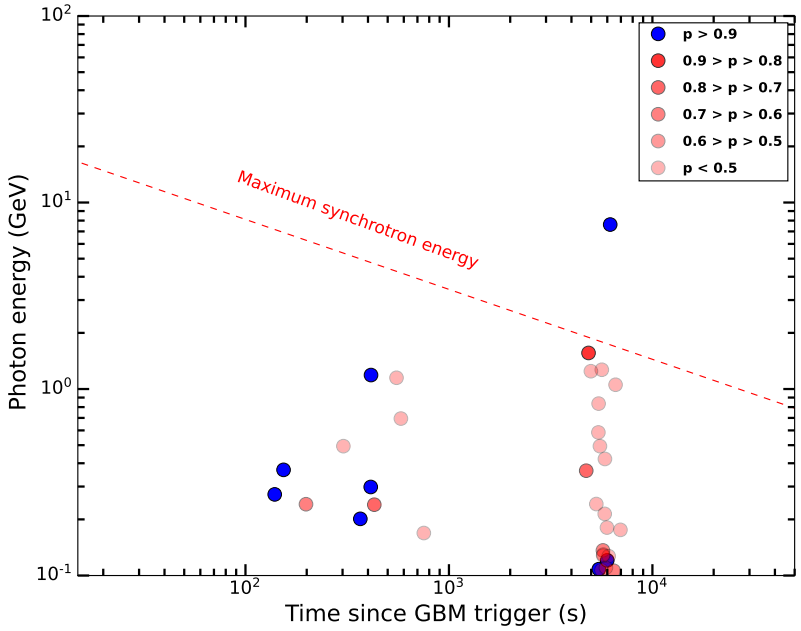

Figure 2: Photons detected by *Fermi*–LAT with their respective energies and probabilities of being associated with GRB 200623A. The maximum energy photon (with $> 90\%$ probability) detected by LAT is 7.56 GeV. The diagonal dashed line represents the theoretical limit of maximum synchrotron energy of electron.

2.2. LAT data

The LAT data was extracted up to 5×10^4 s since the burst from the LAT catalogue. We carried out unbinned likelihood analysis using `GTBurst` software. The energy bin selected for the LAT analysis is 100 MeV–300 GeV, and the maximum zenith angle is chosen 100° to discard photons coming from Earth's limb. As GRB 200613A is a long duration event ($> 10^3$ s), P8R3_SOURCE_V3 was taken as a response. We use `gtsrcprob` task for checking the probability of photons associated with the GRB 200613A. The maximum energetic photon detected by LAT for this event is 7.56 GeV, observed at 6.2 ks since the burst with the probability of association with the source is $> 90\%$. To investigate the origin of the LAT detected photons, we plotted the maximum synchrotron energy possible by photons with the dashed red line in Fig. 2 (Piran and Nakar, 2010; Fraija et al., 2019). All the photons of GRB 200613A detected by LAT are lying below the line following the synchrotron emission except for the maximum energetic photon. This indicates that the 7.56 GeV photon comes from a separate origin.

3. Location of GRB 200613A in the $E_{\rm p}$–$E_{\rm iso}$ and $E_{\rm p}$–T_{90} plots

3.1. $E_{\rm p}$–$E_{\rm iso}$ correlation

A unique property of GRB prompt emission is that the spectral peak energy of the νF_ν spectrum ($E_{\rm p,i}$) and the isotropic equivalent energy of the prompt emission are correlated (Amati, 2006). This correlation is primarily used in prompt emission studies to classify the GRBs

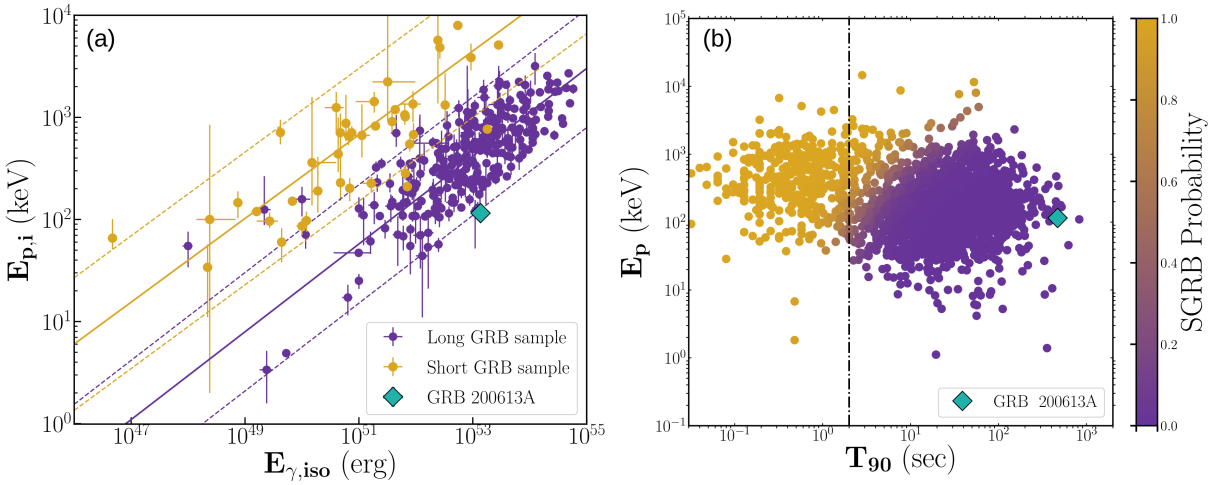

Figure 3: (a) $E_{\rm p}$–$E_{\rm iso}$ and (b) $E_{\rm p}$–T_{90} correlations for the sample of long (purple circles) and short (goldenrod circles) GRBs. In the $E_{\rm p}$–$E_{\rm iso}$ plot, the dashed line in the same colours corresponds to the 3σ scatter of the correlation. The light-green diamond symbol represents the position GRB 200613A in these plots.

and estimate their redshifts if the spectroscopic redshifts are unknown. The correlation observed among different types of investigated gamma-ray transients is supported by empirical evidence indicating a power law relationship. Moreover, these transients exhibit distinct and well-separated regions. Fig. 3a depicts the correlation between 316 short and long GRBs published in Minaev and Pozanenko (2021).

Using the time-integrated fluence value in the 10–1000 keV range and redshift information from the host galaxy observation, the calculated $E_{\gamma,\rm iso}$ value is $(1.37 \pm 0.16) \times 10^{53}$ erg. The spectral peak energy for GRB 200613A, $E_{\rm p,i}$, is $114.90^{+5.00}_{-3.00}$ keV (Table 1). From Fig. 3a, it is evident that GRB 200613A lies beyond the 3σ boundary of the long GRBs.

3.2. $E_{\rm p}$–T_{90} correlation

Another method of classifying the GRBs is spectral hardness and peak energy ($E_{\rm p}$) correlation. To calculate the probability of a GRB being short or long, we used the Bayesian Gaussian Mixture Model (BGMM). Figure 3b shows a bimodal distribution between the peak energy and the T_{90} duration of GRB prompt emission.

The hardness ratio (HR) can be interpreted as the ratio of counts between two energy bands. We considered the 8–50 keV and 50–300 keV bands for our calculation. The calculated value of HR for GRB 200613A is 0.58 ± 0.05. $E_{\rm p}$ is calculated via model fitting of GBM data, which comes to around 115 ± 5 keV (Table 1). We estimated the T_{90} duration of GRB 200613A considering the total emission episodes using GBM data that is 470 ± 5 s. From Fig. 3b, we see that GRB 200613A lies at the extreme end of the duration distribution.

4. Summary

We carried out a comprehensive, prompt emission analysis of GRB 200613A where different parameters such as T_{90}, HR, $E_{\rm p}$, and $E_{\rm iso}$ were estimated. The parameters were compared with a larger sample of GRBs. The burst duration of GRB 200613A suggests that it lies at the boundary of the long and ultra-long duration GRBs. The light curve in 50–300 keV consists of a bright peak emission up to ~ 50 s followed by a weaker emission up to 470 s. However, the evidence of extended emission is not seen in the light curve of the 300–900 keV energy band. The temporal structure of GRB 200613A resembles the ultra-long GRBs. We have also performed time-integrated spectral analysis for the four GBM detectors (NaI0, NaI1, NaI6, BGO0) with the highest count rates, suggesting that the Band function can explain the peak emission (9–17 s). In contrast, the late-time weak extended emission best fits with a power law because of poor count rates. In both the $E_{\rm p}$–$E_{\rm iso}$ and $E_{\rm p}$–T_{90} correlations, this burst is located at the extreme end of the long GRB sample. The isotropic energy ($E_{\rm iso}$) of GRB 200613A estimated from the prompt emission study is $1.37^{+0.05}_{-0.04} \times 10^{53}$ erg, which enlists this GRB in the hyper-energetic GRBs detected by *Fermi*. *Fermi*-LAT detected a 7.56 GeV photon 6.2 ks after the burst trigger, which lies above the maximum synchrotron energy of photons and might come from other origins such as proton synchrotron and synchrotron self-Compton emission (Zhang et al., 2020, 2023).

This study presents the prompt emission properties of GRB 200613A. We have yet to explore the afterglow properties of this burst. However, complete prompt emission and afterglow analysis of GRB 200613A will be useful to provide conclusive information about the progenitor channel, jet properties, emission mechanism, and environment, which will be carried out in future.

Acknowledgments

We thank the referee for providing valuable comments which have improved the presentation and content of the manuscript.

Further Information

Authors' ORCID identifiers

0000-0003-2265-0381 (Ankur GHOSH)
0000-0003-1637-267X (Kuntal MISRA)
0000-0001-9868-9042 (Dimple)

Author contributions

All authors in this work have made significant contributions.

Conflicts of interest

The authors declare no conflict of interest.

References

Acuner, Z., Ryde, F., Pe'er, A., Mortlock, D. and Ahlgren, B. (2020) The fraction of gamma-ray bursts with an observed photospheric emission episode. ApJ, 893(2), 128. https://doi.org/10.3847/1538-4357/ab80c7.

Amati, L. (2006) The $E_{\rm p,i}$–$E_{\rm iso}$ correlation in gamma-ray bursts: updated observational status, re-analysis and main implications. MNRAS, 372(1), 233–245. https://doi.org/10.1111/j.1365-2966.2006.10840.x.

Band, D. L. (1997) Gamma-ray burst spectral evolution through cross-correlations of discriminator light curves. ApJ, 486(2), 928–937. https://doi.org/10.1086/304566.

Bissaldi, E., Lesage, S. and Fermi GBM Team (2020) GRB 200613A: Fermi GBM observation. GCN Circular 27930. https://gcn.nasa.gov/circulars/27930.

Boër, M., Gendre, B. and Stratta, G. (2015) Are ultra-long gamma-ray bursts different? ApJ, 800(1), 16. https://doi.org/10.1088/0004-637X/800/1/16.

Burgess, J. M., Bégué, D., Greiner, J., Giannios, D., Bacelj, A. and Berlato, F. (2020) Gamma-ray bursts as cool synchrotron sources. NatAs, 4, 174–179. https://doi.org/10.1038/s41550-019-0911-z.

de Ugarte Postigo, A., Kann, D. A., Thoene, C. C., Blazek, M. and Agui Fernandez, J. F. (2021) GRB 200613A: Host galaxy redshift from OSIRIS/GTC. GCN Circular 29320. https://gcn.nasa.gov/circulars/29320.

Fermi GBM Team (2020) GRB 200613A: Fermi GBM final real-time localization. GCN Circular 27926. https://gcn.nasa.gov/circulars/27926.

Fraija, N., Dichiara, S., Pedreira, A. C. C. d. E. S., Galvan-Gamez, A., Becerra, R. L., Barniol Duran, R. and Zhang, B. B. (2019) Analysis and modeling of the multi-wavelength observations of the luminous GRB 190114C. ApJ, 879(2), L26. https://doi.org/10.3847/2041-8213/ab2ae4.

Kass, R. E. and Rafferty, A. E. (1995) Bayes factors. J. Am. Stat. Assoc., 90, 773–795. https://doi.org/10.1080/01621459.1995.10476572.

Komatsu, E., Smith, K. M., Dunkley, J., Bennett, C. L., Gold, B., Hinshaw, G., Jarosik, N., Larson, D., Nolta, M. R., Page, L., Spergel, D. N., Halpern, M., Hill, R. S., Kogut, A., Limon, M., Meyer, S. S., Odegard, N., Tucker, G. S., Weiland, J. L., Wollack, E. and Wright, E. L. (2011) Seven-year *Wilkinson Microwave Anisotropy Probe* (*WMAP*) observations: Cosmological interpretation. ApJS, 192, 18. https://doi.org/10.1088/0067-0049/192/2/18.

Kouveliotou, C., Meegan, C. A., Fishman, G. J., Bhat, N. P., Briggs, M. S., Koshut, T. M., Paciesas, W. S. and Pendleton, G. N. (1993) Identification of two classes of gamma-ray bursts. ApJ, 413, L101–L104. https://doi.org/10.1086/186969.

Levan, A. J., Tanvir, N. R., Starling, R. L. C., Wiersema, K., Page, K. L., Perley, D. A., Schulze, S., Wynn, G. A., Chornock, R., Hjorth, J., Cenko, S. B., Fruchter, A. S., O'Brien, P. T., Brown, G. C., Tunnicliffe, R. L., Malesani, D., Jakobsson, P., Watson, D., Berger, E., Bersier, D., Cobb, B. E., Covino, S., Cucchiara, A., de Ugarte Postigo, A., Fox, D. B., Gal-Yam, A., Goldoni, P., Gorosabel, J., Kaper, L., Krühler, T., Karjalainen, R., Osborne, J. P., Pian, E., Sánchez-Ramírez, R., Schmidt, B., Skillen, I., Tagliaferri, G., Thöne, C., Vaduvescu, O., Wijers, R. A. M. J. and Zauderer, B. A. (2014) A new population of ultra-long duration gamma-ray bursts. ApJ, 781(1), 13. https://doi.org/10.1088/0004-637X/781/1/13.

Minaev, P. Y. and Pozanenko, A. S. (2021) Erratum: The $E_{\rm p,i}$–$E_{\rm iso}$ correlation: type I gamma-ray bursts and the new classification method. MNRAS, 504(1), 926–927. https://doi.org/10.1093/mnras/stab1031. Correction to https://doi.org/10.1093/mnras/stz3611.

Ohno, M., Kovacevic, M., Bissaldi, E., Axelsson, M., Longo, F. and Fermi-LAT Collaboration (2020) GRB 200613A: Fermi-LAT detection. https://gcn.nasa.gov/circulars/27931.

Piran, T. and Nakar, E. (2010) On the external shock synchrotron model for gamma-ray bursts' GeV emission. ApJ, 718(2), L63–L67. https://doi.org/10.1088/2041-8205/718/2/L63.

Stratta, G., Gendre, B., Atteia, J. L., Boër, M., Coward, D. M., De Pasquale, M., Howell, E., Klotz, A., Oates, S. and Piro, L. (2013) The ultra-long GRB 111209A. II. Prompt to afterglow and afterglow properties. ApJ, 779(1), 66. https://doi.org/10.1088/0004-637X/779/1/66.

Vianello, G., Lauer, R. J., Burgess, J. M., Ayala, H., Fleischhack, H., Harding, P., Hui, M., Marinelli, S., Savchenko, V. and Zhou, H. (2017) The Multi-Mission Maximum Likelihood framework (3ML). In Proceedings of the 7th International Fermi Symposium, vol. 312 of *PoS*. https://doi.org/10.22323/1.312.0130.

Zhang, B.-B., Zhang, B., Murase, K., Connaughton, V. and Briggs, M. S. (2014) How long does a burst burst? ApJ, 787(1), 66. https://doi.org/10.1088/0004-637X/787/1/66.

Zhang, B. T., Murase, K., Ioka, K., Song, D., Yuan, C. and Mészáros, P. (2023) External inverse-compton and proton synchrotron emission from the reverse shock as the origin of VHE gamma rays from the hyper-bright GRB 221009A. ApJ, 947(1), L14. https://doi.org/10.3847/2041-8213/acc79f.

Zhang, H., Christie, I. M., Petropoulou, M., Rueda-Becerril, J. M. and Giannios, D. (2020) Inverse compton signatures of gamma-ray burst afterglows. MNRAS, 496(1), 974–986. https://doi.org/10.1093/mnras/staa1583.